Available online at www.sciencedirect.com
ScienceDirect
Journal of Power Sources 175 (2008) 464–472
JOURNAL OF POWER SOURCES
www.elsevier.com/locate/jpowsour

Liquid hydrogen production via hydrogen sulfide methane reformation

Cunping Huang*, Ali T-Raissi

University of Central Florida, Florida Solar Energy Center, 1769 Clearlake Road, Cocoa, FL 32922, United States

Received 4 September 2007; received in revised form 20 September 2007; accepted 21 September 2007
Available online 3 October 2007

Abstract

Hydrogen sulfide (H_2S) methane (CH_4) reformation (H_2SMR) ($2H_2S + CH_4 = CS_2 + 4H_2$) is a potentially viable process for the removal of H_2S from sour natural gas resources or other methane containing gases. Unlike steam methane reformation that generates carbon dioxide as a by-product, H_2SMR produces carbon disulfide (CS_2), a liquid under ambient temperature and pressure—a commodity chemical that is also a feedstock for the synthesis of sulfuric acid. Pinch point analyses for H_2SMR were conducted to determine the reaction conditions necessary for no carbon lay down to occur. Calculations showed that to prevent solid carbon formation, low inlet CH_4 to H_2S ratios are needed. In this paper, we analyze H_2SMR with either a cryogenic process or a membrane separation operation for production of either liquid or gaseous hydrogen. Of the three H_2SMR hydrogen production flowsheets analyzed, direct liquid hydrogen generation has higher first and second law efficiencies of exceeding 80% and 50%, respectively.

Keywords: Hydrogen sulfide; Hydrogen sulfide methane reformation; Cryogenic separation; Liquid hydrogen production

1. Introduction

Hydrogen sulfide (H_2S) is a common contaminant in many of the world's natural gas (NG) wells. Approximately one-third of US NG resources can be considered as low or sub-quality gas not suited for pipeline shipment [1]. H_2S concentration in NG varies from traces to 90% by volume [2]. In natural gas processing H_2S is viewed as a pollutant because it corrodes pipelines and deactivates metal-based catalysts used in steam methane reformation (SMR). There is a number of hydrogen sulfide removal processes practiced commercially or in bench scale demonstrations. Based on the H_2S reactions involved, these technologies can be separated into three categories:

$$\text{partial oxidation: } H_2S + 0.5O_2 = S + H_2O, \quad \Delta H^\circ_{298\,\mathrm{K}} = -265.2\,\mathrm{kJ\,mol^{-1}} \tag{1}$$

$$\text{decomposition: } H_2S = 0.5S_2 + H_2, \quad \Delta H^\circ_{298\,\mathrm{K}} = 79.9\,\mathrm{kJ\,mol^{-1}} \tag{2}$$

$$\text{reformation: } 2H_2S + CH_4 = CS_2 + 4H_2, \quad \Delta H^\circ_{298\,\mathrm{K}} = 232.4\,\mathrm{kJ\,mol^{-1}} \tag{3}$$

$\Delta H^\circ_{298\,\mathrm{K}}$ for Reaction (1) is calculated from the formation enthalpies of liquid water and gaseous hydrogen sulfide:

$$\Delta H^\circ_{298\,\mathrm{K}} = \Delta H^\circ_{\mathrm{f}\,298\,\mathrm{K,\ liquid\ water}} - \Delta H^\circ_{\mathrm{f}\,298\,\mathrm{K,\ gaseous\ hydrogen\ sulfide}} = -285.8 + 20.6 = -265.2\,\mathrm{kJ\,mol^{-1}}$$

Kohl and Nielsen [3] summarized in detail the commercially available H_2S partial oxidation processes, including Claus plants and liquid phase oxidation processes. The first step of partial oxidation of H_2S (Reaction (1)) is to convert S^{2-} to S^{4+} generating sulfur dioxide (SO_2) ($\Delta H^\circ_{\mathrm{f}\,SO_2,\,\mathrm{gas}} = -296.81\,\mathrm{kJ\,mol^{-1}}$) as a reaction intermediate. In a Claus plant, a portion of H_2S is oxidized to form SO_2, which then further oxidizes the remaining H_2S to produce elemental sulfur and water as follows

$$H_2S + 1.5O_2 = H_2O + SO_2 \tag{4}$$

$$2H_2S + SO_2 = 2H_2O + 3S \tag{5}$$

---

* Corresponding author. Tel.: +1 321 638 1505; fax: +1 321 638 1010.
E-mail address: chuang@fsec.ucf.edu (C. Huang).

0378-7753/$ – see front matter © 2007 Elsevier B.V. All rights reserved.
doi:10.1016/j.jpowsour.2007.09.079

Nomenclature

CE	cooling energy requirement for coolers
CompE	compressor energy requirement
CondE	condenser energy input for distillation column
ExpE	expander energy requirement
HE	energy requirement for heaters
HX	heat exchanger
RebE	re-boiler energy input for distillation column

Greek letters

η_{1st}	first law efficiency
η_{2nd}	second law efficiency

The overall reaction is partial oxidation of H_2S according to Reaction (1). In this process only elemental sulfur and thermal heat can be generated from H_2S and no H_2 is produced. The major issue in the Claus process is the removal of SO_2 from tail gas. Generation of SO_2 in the tail gas is due to the fact that excess SO_2 is needed to complete Reaction (5). In addition to the Claus process, partial oxidation of H_2S can also be realized via aqueous redox systems that consist of two steps: (1) H_2S scrubbing during which H_2S is oxidized to elemental sulfur and (2) oxidation of a redox pair by air or oxygen. The net reaction products for the H_2S partial oxidization are sulfur and water. One example involving the use of Fe^{2+}/Fe^{3+} redox system is shown as follows

$$2Fe^{3+}(aq) + H_2S(g) = 2Fe^{2+}(aq) + S(c) + 2H^{+}(aq) \qquad (6)$$

$$2Fe^{2+}(aq) + (1/2)O_2(g) + H_2O(l) = 2Fe^{3+}(aq) + 2OH^{-}(aq) \qquad (7)$$

Typical anions used above include Cl^- and $SO_4{}^{2-}$ or organic reagents, chelates, cyanide, etc.

H_2S decomposition (Reaction (2)), on the other hand, is an endothermic process that can be carried out in a variety of ways, including direct thermal decomposition, thermochemical cycles, electrochemical or photochemical methods. Some examples are given below:

- High temperature pyrolysis:

  $$H_2S + \text{heat} = H_2 + (1/2)S_2, \quad T > 1500\,^{\circ}C$$

- $FeCl_2$–$FeCl_3$–HCl system [4]:

  $$H_2S(g) + 2FeCl_3(aq) = 2FeCl_2(aq) + 2HCl(aq) + S(c)$$

  $$2FeCl_2(aq) + 2HCl(aq) + \text{electricity} = H_2(g) + 2FeCl_3(aq)$$

- High temperature electrolysis [5]:
  - Cathode:
    $H_2S + 2e^- = S^{2-} + H_2$
  - Anode:
    $S^{2-} = (1/2)S_2 + 2e^-$
- I^-/IO^{3-} system [6,7]:

  $$I^-(aq) + 3H_2O = IO^{3-}(aq) + 3H_2(g) \quad (pH > 13)$$

  $$3H_2S(aq) + IO^{3-}(aq) = 3S(s) + 3H_2O + I^-(aq)$$

- Photochemical process [8–10]:
  - Hydrogen evolution:
    $2HS^- + 2h\nu = H_2(g) + S_2{}^{2-}(aq)$ (photolysis)
  - Sulfur precipitation:
    $S_2{}^{2-}(aq) + H_2S(aq) = S(s) + 2HS^-(aq)$

An excellent review of this topic can be found in Ref. [5]. Huang and T-Raissi [11,12] have also provided a brief review of these technologies, with focus on using H_2S methane reformation (H_2SMR) (Reaction (3)) for the removal of high concentrations of H_2S from low quality natural gas. It should be noted that separation of H_2S from methane (CH_4) is an energy intensive process. In a high H_2S content (sour) NG, H_2S concentration can be as high as 90% making H_2S separation uneconomical. However, as with H_2O in the steam methane reformation (SMR) reaction:

$$2H_2O + CH_4 = 4H_2 + CO_2, \quad \Delta H^{\circ}_{298\,K} = 165.2\,kJ\,mol^{-1} \qquad (8)$$

H_2S can react with methane, according to Reaction (3), producing not only 4 mol of hydrogen, but also 1 mol of carbon disulfide (CS_2), a valuable product that is more desirable than elemental sulfur as a feedstock for the production of sulfuric acid (H_2SO_4). Furthermore, CS_2 can be hydrogenated to produce gasoline–range hydrocarbon liquid fuels [13] as follows

$$CS_2 + 3H_2 = –[CH_2]– + 2H_2S \qquad (9)$$

Unlike SMR, H_2SMR does not generate any greenhouse gases. As described above, one typical application of H_2SMR would be to remove H_2S from sub-quality natural gases (SQNGs) containing high concentrations of H_2S. Few technologies are currently available for the economical removal of high concentration H_2S from natural gas. A conceptual process [11,12] has been proposed that consists of the following two steps: (1) SMR in the presence of H_2S and (2) H_2SMR to generate hydrogen and CS_2. No H_2S separation from hydrocarbons is therefore necessary in this process.

It is noted that, compared to partial oxidation and decomposition of H_2S (Reactions (1) and (2)), H_2SMR is a less explored process. One objective of this paper is to assess the merits of H_2SMR from thermodynamic and chemical equilibrium considerations, utilizing pinch point analyses to determine conditions needed for the zero carbon lay down. Only when no solid carbon is generated can H_2SMR be beneficial in terms of resolving catalyst deactivation issues. In this paper, the thermodynamic analyses of H_2SMR were carried out using a Gibbs reactor in AspenPlus^{TM} chemical process simulation (CPS). Another objective of this paper is to develop flowsheets for the production of gaseous H_2 and/or liquid H_2 (LH_2) using H_2SMR. HYSYS^{TM} CPS was employed to determine the total energy requirement needed to calculate the overall process efficiencies. Two types of flowsheets, membrane separation and cryogenic process including cryogenic separation and H_2 liquefaction, were developed and process efficiencies were calculated.

2. Thermodynamics of hydrogen sulfide reforming of methane (H_2SMR)

2.1. Chemical equilibrium calculations for H_2SMR

H_2SMR (Reaction (3)) proceeds via H_2S thermal decomposition (Reaction (2)) and methane pyrolysis according to Reaction (10):

$$CH_4(g) = C(s) + 2H_2(g), \quad \Delta H^{\circ}_{298K} = 74.9\,\mathrm{kJ\,mol^{-1}} \qquad (10)$$

Reactions (2) and (10) both require high temperatures and a catalyst in order to increase the reaction rate. In Reaction (2) gaseous sulfur does not normally deactivate the metal sulfide-based catalyst used in H_2SMR. However, solid carbon, if formed due to Reaction (10), will foul the catalyst surface and cause its deactivation. Therefore, to carry out H_2SMR requires reaction conditions such that no carbon lay down occurs. In this paper, the thermodynamics and chemical equilibrium compositions of H_2SMR were carried out using a Gibbs reactor unit operation in the AspenPlus^{TM} CPS. The reaction temperatures and concentrations at which there is no carbon generated are termed as pinch point parameters. The conversion and yields for Reactions (2), (3) and (10) are defined as follows.

CH_4 and H_2S conversions are defined by Eqs. (a) and (b), respectively:

$$CH_4\,(\%) = \frac{[CH_4]_0 - [CH_4]}{[CH_4]_0} \times 100 \qquad (a)$$

$$H_2S\,(\%) = \frac{[H_2S]_0 - [H_2S]}{[H_2S]_0} \times 100 \qquad (b)$$

where $[CH_4]_0$ and $[H_2S]_0$ denote the initial (input) concentrations of CH_4 and H_2S, respectively. $[CH_4]$ and $[H_2S]$ are equilibrium concentrations of CH_4 and H_2S at the reactor outlet, respectively. Yields of reaction products are defined based on the moles of products generated divided by the total number of moles of input reactants. Yields of H_2, CS_2, S_2 gas and solid carbon (soot) are given as follows

$$H_2\,(\%) = \frac{[H_2]}{2[CH_4]_0 + [H_2S]_0} \times 100 \qquad (c)$$

$$CS_2\,(\%) = \frac{[CS_2]}{[CH_4]_0} \times 100 \qquad (d)$$

$$S_2\,(\%) = \frac{2[S_2]}{[H_2S]_0} \times 100 \qquad (e)$$

$$C\,(\%) = \frac{[C]}{[CH_4]_0} \times 100 \qquad (f)$$

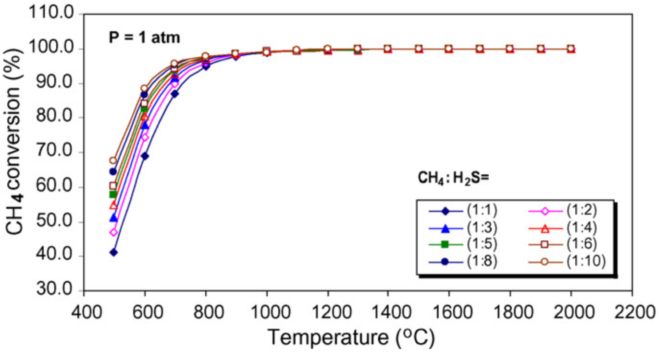

Fig. 1. Methane conversion at various temperatures and CH_4 to H_2S molar feed ratios.

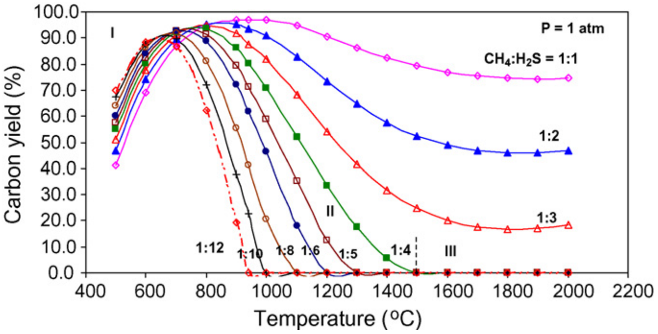

Fig. 2. Yield of carbon as a function of temperature and CH_4 to H_2S molar feed ratios (I: CH_4 pyrolysis; II: CH_4 pyrolysis and H_2SMR; III: H_2SMR).

where $[X]_0$ and $[X]$ denote the initial and equilibrium molar concentrations for species X, respectively. Chemical equilibria based on the principle of minimization of Gibbs free energy in the course of H_2SMR are depicted in Figs. 1–6. These results provide useful data for selecting reaction conditions and constructing process flowsheets.

2.2. Methane conversion and yields of carbon and carbon disulfide

The major factor influencing CH_4 conversion is temperature. Fig. 1 shows that CH_4 conversion reaches 100% as the reaction temperatures become greater than 800 °C for CH_4 to H_2S ratio, x (defined as: $[CH_4]_0/[H_2S]_0$) ranging from 1 to 0.1. Fig. 2 depicts carbon lay down as a function of temperature. It is noted that car-

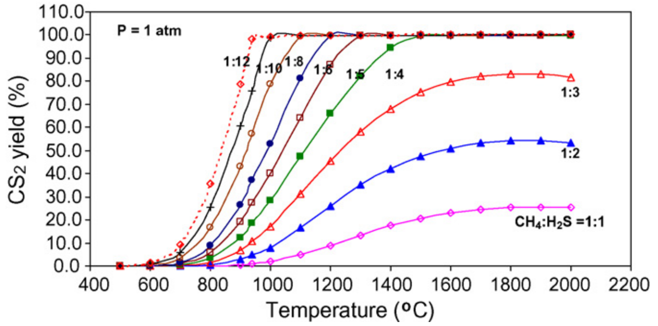

Fig. 3. Yield of carbon disulfide as a function of temperature and CH_4 to H_2S molar feed ratios.

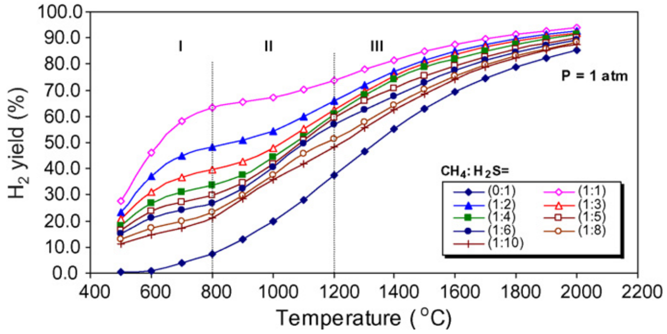

Fig. 4. Hydrogen yields as a function of temperature and CH_4 to H_2S molar feed ratios (I: CH_4 pyrolysis; II: CH_4 and H_2S pyrolysis and H_2SMR; III. H_2SMR and H_2S pyrolysis).

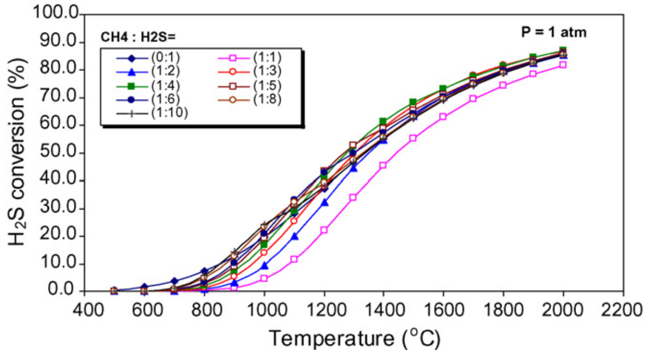

Fig. 5. H_2S conversion as a function of temperature and CH_4 to H_2S molar feed ratios.

bon yield increases with increasing temperature until the yield reaches a maximum value, and then drops with further increase in the temperature. When x is lower than 0.25 no free carbon is formed at reaction temperatures higher than a pinch point temperature, which is defined as the lowest temperature at which solid carbon is formed. According to Fig. 2, pinch point temperature decreases as x values decrease. For example, at $x = 0.25$, the pinch point temperature is 1500 °C, while it is 1000 °C at $x = 0.1$. No pinch point exists if the feed ratio x is greater than 0.25, indicating that carbon lay down cannot be avoided at any temperature if the feed ratio $x = [CH_4]_0/[H_2S]_0 > 0.25$. Thermodynamic calculations show that in order to prevent carbon formation, a greater than stoichiometric amount of H_2S is required. In the hydrogen production process excess H_2S can serve as a working fluid and can be re-circulated.

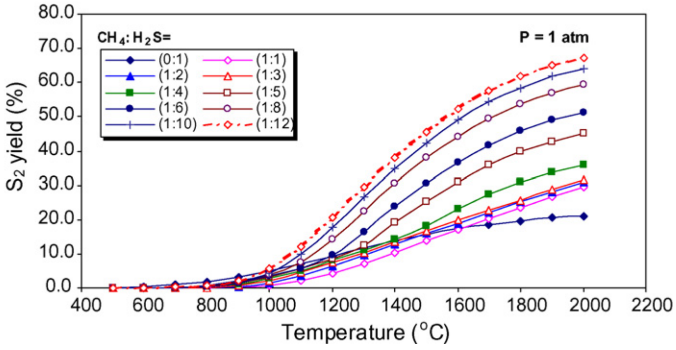

Fig. 6. Yield of S_2 gas as a function of temperature and CH_4 to H_2S molar feed ratios.

The pinch point analysis provides a tool for the optimization of process energy as well as for the interpretation of reaction mechanisms. Based upon the yield of carbon (Fig. 2), sulfur (Fig. 6) and CH_4 conversions (Fig. 1), the reaction mechanisms involved in H_2SMR can be interpreted. As discussed previously, three reactions are involved in the course of H_2SMR (Reactions (2), (3) and (10)). Therefore, three temperature ranges can be distinguished as follows:

(I) Lower than the maximum carbon lay down temperature.
(II) Between maximum carbon lay down temperature and the pinch point temperature.
(III) Above the pinch point temperature.

In the first temperature range, carbon is produced by CH_4 pyrolysis via Reaction (10). At these temperatures the yield of carbon disulfide (CS_2) approaches zero (Fig. 3), which can also be explained in terms of the H_2 yields as depicted in Fig. 4. For example, at $x = 0.5$, the maximum carbon yield occurs at 800 °C, at which the CS_2 yield approaches zero. This result indicates that any H_2 produced originates from CH_4 decomposition. Temperature range II is a transition zone at which both Reactions (2) and (10) occur simultaneously. However, when the temperature is higher than the pinch point temperature (temperature range III), no free carbon is formed and the CH_4 conversion is 100% as shown in Fig. 1, suggesting that CH_4 is completely reformed by H_2S to H_2 and CS_2. Furthermore, as shown in Figs. 3 and 5, the yield of CS_2 and H_2S conversion increase as the temperature increases. Because there is sulfur formed at temperature zone III (Fig. 6), the mechanism of H_2SMR in this regime must involve both H_2S decomposition and reformation instead of CH_4 pyrolysis. Therefore, in the temperature range III, H_2SMR is accompanied by the Reaction (2), that is H_2S pyrolysis. Finally, it appears that H_2S decomposition cannot be avoided and increases as the x values decrease.

2.3. *Hydrogen sulfide conversion and yields of hydrogen and S_2*

At any temperature, H_2S conversion (Fig. 5) is less than that of CH_4 (Fig. 1), especially at temperatures below 1000 °C wherein H_2S conversion is less than 20%. At temperatures below 1000 °C, the feed ratio x does not affect H_2S conversion significantly. H_2S decomposition is the limiting step in the H_2SMR process as it proceeds by the sequential reaction involving H_2S pyrolysis to form sulfur diatomic gas (S_2) (Reaction (2)), followed by S_2 reaction with CH_4 to produce carbon disulfide (CS_2) and H_2 ($S_2 + CH_4 = CS_2 + 2H_2$). Figs. 4 and 6 depict the yield of H_2 and S_2, respectively. As compared with the yield of carbon (Fig. 2), H_2 yield (Fig. 4) reveals three distinct temperature ranges similar to those shown in Fig. 2 as follows:

(I) H_2 production via CH_4 pyrolysis that occurs at low to intermediate temperature range ($T < 800\,°C$).
(II) H_2 production via methane pyrolysis and H_2SMR process ($800\,°C < T < 1200\,°C$).
(III) H_2 production via both H_2SMR and H_2S decomposition process ($T > 1200\,°C$).

In temperature range I (Fig. 4), H_2 yield increases rapidly as the temperature increases, implying that CH_4 pyrolysis is a thermodynamically favored reaction as the temperatures increase. In the transition temperature range II, the mechanism by which hydrogen is produced changes from methane decomposition to H_2SMR, resulting in a lower hydrogen yield. In the high temperature range III, the rate of hydrogen production increases but is still lower than that in the lower temperature range I. The fact that hydrogen yield increases in range III as temperature is increased indicates that higher temperatures favor the decomposition of both H_2SMR and H_2S. Hydrogen yields are also a function of the methane to hydrogen sulfide feed ratio x. As the x ratio increases, the yield of hydrogen drops significantly. Based on the results of Figs. 1–6, it can be concluded that as the reaction temperature increases, methane pyrolysis is the dominant reaction, giving way to H_2SMR at higher temperatures. At reaction temperatures exceeding 1200 °C, H_2S decomposition becomes the main mechanism by which H_2 is generated. Furthermore, comparing Figs. 2 and 6, it can be seen that there are no pinch point temperatures for which both the carbon and S_2 yields are zero, suggesting that the production of S_2 cannot be avoided. For example, at feed ratio $x = [CH_4]_0/[H_2S]_0 = 1/4$, the temperature at which carbon lay down is zero (pinch point temperature) is calculated to be above 1500 °C (see Fig. 2). At temperatures above 1500 °C, S_2 yield increases from 20% at 1500 °C to about 35% at 2000 °C. However, S_2 generated at high temperature is in gaseous form, and its impact on the metal sulfide catalysts is minimal.

2.4. H_2SMR energy requirements

Under isothermal conditions, H_2SMR total process enthalpy changes, shown in Fig. 7, were calculated as follows

$$\Delta H_{\text{Total}} = \sum_i (\Delta H)_{\text{Products}} - \sum_j (\Delta H)_{\text{Reactants}} \tag{g}$$

where the reactants are hydrogen sulfide and methane, and reaction products are hydrogen, carbon disulfide, carbon, sulfur diatomic gas and the un-reacted hydrogen sulfide and methane. Fig. 7 shows that ΔH_{Total} is a strong function of both the temperature and the CH_4 to H_2S feed ratio, x. As discussed previously, an H_2SMR process consists of three major reactions: CH_4 decomposition, H_2SMR and H_2S decomposition. However, enthalpy changes of these three reactions depend upon the isothermal temperature and x. Since the extents (or conversions) of these reactions are different, the enthalpy changes will also differ from the standard reaction enthalpies, $\Delta H^{\circ}_{298\,\text{K}}$. In the course of H_2SMR, methane decomposition can be completed at temperatures higher than 800 °C (Fig. 1). However, H_2S does not completely decompose to H_2 and S_2 even at temperatures exceeding 2000 °C. Furthermore, H_2S decomposition is insensitive to x (Fig. 5). The extent of H_2SMR, on the other hand, can be measured from the yield of CS_2. As shown in Fig. 3, CS_2 yields depend not only on the temperature, but also on the feed ratio x. In short, the total enthalpy change of the H_2SMR process is dependant on the type and extent of the reactions involved.

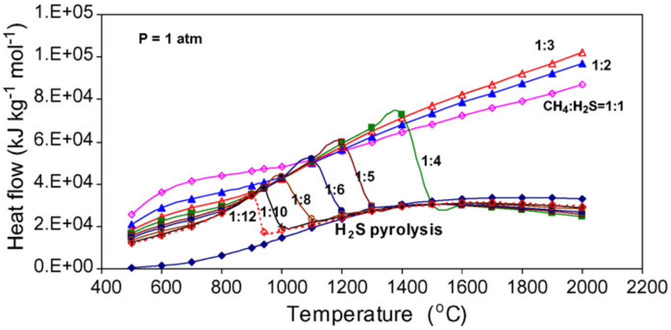

Fig. 7. Total heat flow for the H_2SMR as a function of temperature and CH_4 to H_2S molar feed ratios.

As shown in Fig. 7, the total enthalpy change of an H_2SMR process can be divided into two parts. The higher enthalpy level refers to the energy needed to carry out both CH_4 decomposition and H_2SMR. The lower enthalpy level is mainly for H_2SMR and a small portion for the H_2S decomposition due to low H_2S conversion. Note that at pinch point temperatures the total enthalpy changes jump from the higher enthalpy level to the lower one, at which point a major part of the overall energy input is shifted from the combination of CH_4 decomposition and H_2SMR to mostly H_2SMR. The reduction of total energy requirement indicates that avoiding carbon lay down (due to methane decomposition) is also beneficial in terms of minimizing the overall process energy requirement. As shown in Fig. 7, H_2SMR is a highly endothermic process, making it a good candidate for utilization of a high temperature heat source, such as a concentrating solar furnace, for efficient hydrogen production. Fig. 8 illustrates the pinch point temperature and thermal energy requirement as a function of inlet H_2S to CH_4 ratio, $1/x$. The results show that as x decreases, the pinch point temperature also decreases, as does the total heat flow required for carrying out H_2SMR.

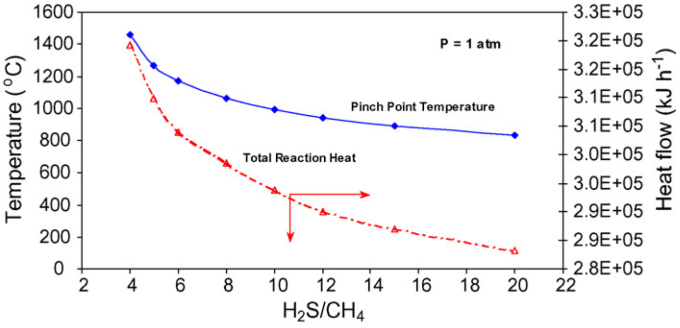

Fig. 8. Pinch point temperatures and total heat flow as a function of H_2S to CH_4 molar feed ratios.

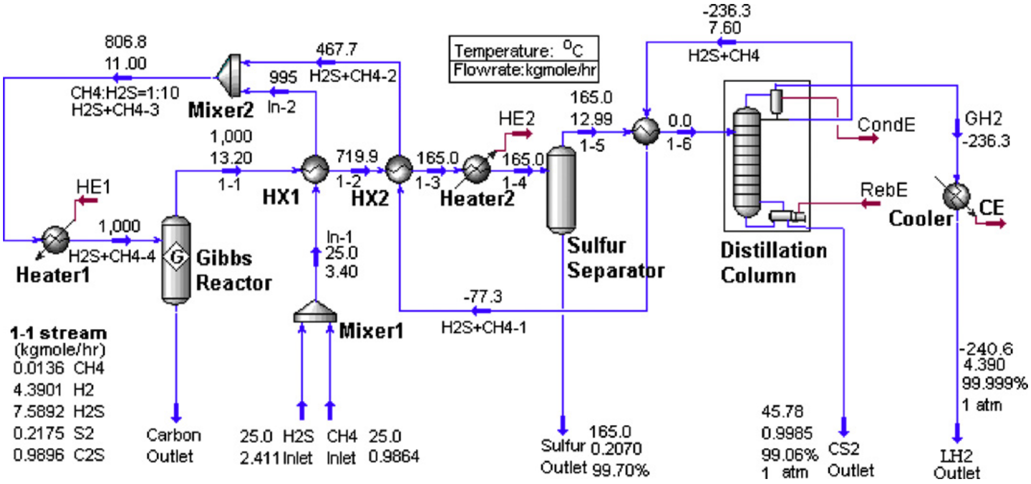

Fig. 9. Flowsheet depicting liquid hydrogen production via H_2SMR.

3. Process flowsheet for hydrogen production via H_2SMR

3.1. Process flowsheet

Based on the thermodynamic analyses above, three flowsheets (Figs. 9–11) were established for either liquid or gaseous hydrogen production using H_2SMR operated at pinch point conditions. The total energy requirement and material balance for this process can be determined based on the unit operations involved in the flow diagrams.

The flow diagram for liquid hydrogen production is shown in Fig. 9. Hydrogen, sulfur diatomic gas and carbon disulfide are produced within a Gibbs reactor. To avoid the formation of solid carbon the feed stream is comprised of a mixture of methane and hydrogen sulfide, with the feed ratio x determined by pinch point analyses. The reaction temperature selected is the pinch point temperature according to our previous thermodynamic analyses. The gaseous mixture at the outlet of the Gibbs reactor is cooled to knock out sulfur. The remaining gas mixture is then sent to a cryogenic distillation column where it is separated into three streams: low temperature (at −236.3 °C), high purity gaseous hydrogen, liquid form carbon disulfide (at 45.78 °C) and a mixture of hydrogen sulfide and methane (at −236.3 °C). After separation, cryogenic energy in the mixture of un-reacted hydrogen sulfide and methane is recovered via heat exchangers. The mixture is then combined with the initial feed stream containing a mixture of hydrogen sulfide and methane. The initial feed ratio x of methane to hydrogen sulfide is kept constant during the process by balancing the consumption and input gases. The gas mixture is then heated and sent back to the Gibbs reactor to complete the cycle. As noted previously, excess hydrogen sulfide in the process serves as a working fluid for the cryogenic separation process so that no other working fluid, such as nitrogen or helium, is required.

The total energy requirement for the entire process consists of two parts: energy required to carry out H_2SMR, ΔH (calculated from a Gibbs reactor (Fig. 7)), and that needed to perform other unit operations included in the flow diagram. The latter can be calculated from the sum of heat exchanges HE1 and HE2, cryogenic distillation energy requirements for condensation CondE, re-boiling RebE, and hydrogen liquefaction CE.

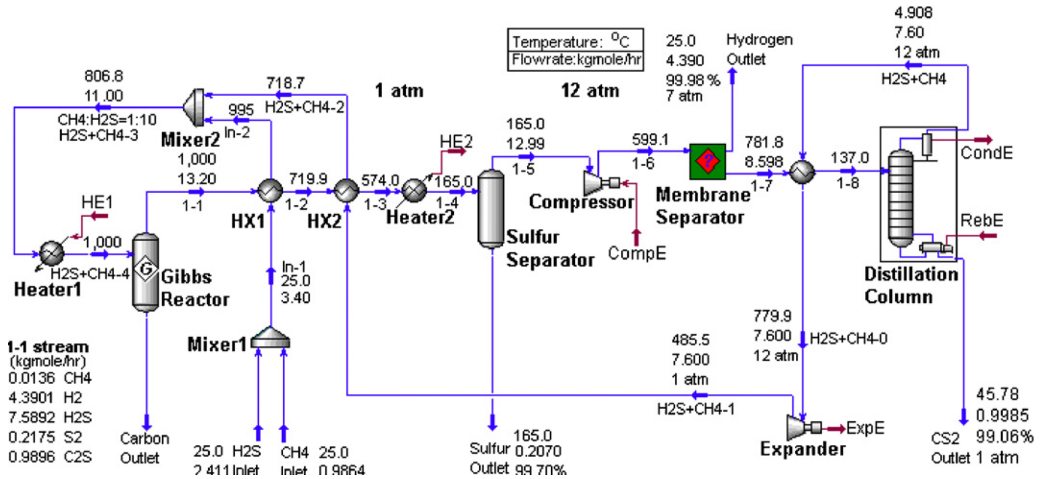

Fig. 10. Flowsheet depicting gaseous hydrogen production via H_2SMR and membrane separation (Type I).

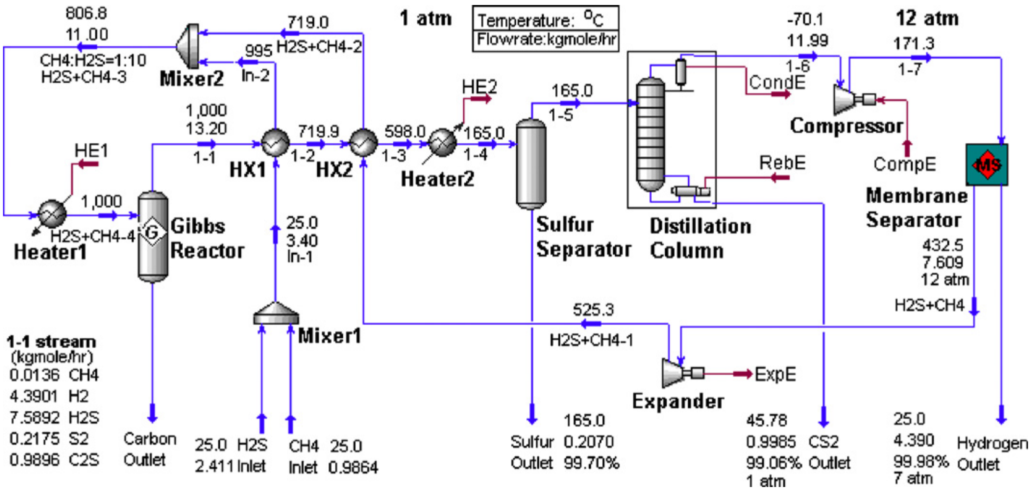

Fig. 11. Flowsheet depicting gaseous hydrogen production via H_2SMR and membrane separation (Type II).

Fig. 9 also shows detailed material balances, indicating that when 0.99 mol of methane and 2.41 mol of hydrogen sulfide have been consumed, 4.39 mol of liquid hydrogen, 0.99 mol of carbon disulfide and 0.21 mol of sulfur have been generated. This result shows that 0.22 mol of hydrogen are produced from decomposition of hydrogen sulfide and 4.18 mol from H_2SMR. Because no solid carbon is generated in this process none of the hydrogen produced is from methane decomposition. We note that this flow diagram incorporates the thermodynamic data from the Gibbs reactor data in the AspenPlus into the HYSYS flowsheet. The Gibbs reactor in the flow diagram was built as a black box with data derived from the AspenPlus database.

Membrane separation can be used to separate gaseous hydrogen from a mixture. Two options for membrane separation in H_2SMR processes are shown in Fig. 10 (type I) and Fig. 11 (type II). Fig. 10 depicts the type I process, in which hydrogen is separated from the gaseous mixture first. After quenching the gas exiting from the Gibbs reactor, sulfur is collected and the remaining gaseous mixture is compressed to 12 atm to allow hydrogen permeation through the membrane. After H_2 is separated, the mixture containing H_2S, CH_4 and CS_2 is sent to a distillation tower to separate CS_2. Afterwards the gas is allowed to expand to 1 atm, mixed with the feed stream, and recycled back to the Gibbs reactor. The membrane separation efficiency for both types is assumed to be 100%.

Type II process is shown in Fig. 11. CS_2 is separated from the gaseous mixture containing H_2S, CH_4 and H_2 from a distillation column. These gases are compressed to 12 atm to allow H_2 to permeate through a membrane, while the H_2S and CH_4 mixed stream is expanded and recycled back to the Gibbs reactor. If liquid hydrogen is required as the final product, extra liquefaction energy is needed to liquefy the gaseous H_2 to LH_2. In this case one more cryogenic cooling step must be added to the process. Results show that the type II process is energetically more efficient than type I because the CS_2 compression and separation in Fig. 10 consumes large amounts of energy. The following energy and efficiency calculations are based on the type II process depicted in Fig. 11.

3.2. Total process energy requirements

The total energy required for the process derives from two contributions: (I) energy needed to carry out the H_2SMR reaction and (II) process energy, including heating, cooling and separation. In the case of membrane separation, compression energy is required in order to separate hydrogen from a gaseous mixture. Note that the energy required for separating hydrogen from its gas mixture is neglected in this calculation. Note also that in the conversion of thermal heat energy to mechanical energy, Carnot efficiency must be taken into account. We assumed 50% conversion efficiency for thermal heat to electrical energy used in the cryogenic separation unit operation. Fig. 12 depicts the overall energy requirements for hydrogen production via H_2SMR for three scenarios involving gaseous or liquid hydrogen production combined with membrane or cryogenic separation processes. The results show that total energy required for LH_2 production via a cryogenic separation process is the lowest at all inlet hydrogen sulfide to methane ratios (1/*x*).

The cryogenic separation process (Fig. 9) integrates hydrogen separation and liquefaction in one process. The advantages of this approach are as follows:

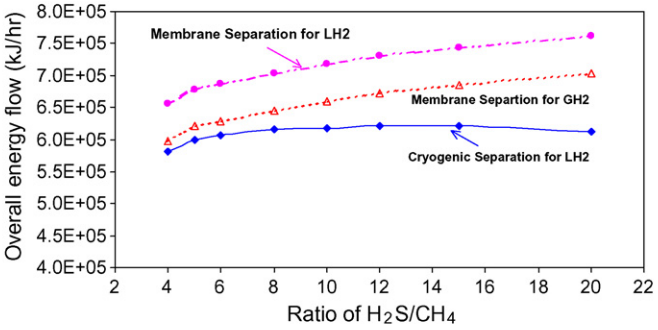

Fig. 12. Overall energy requirements for hydrogen production via H_2SMR.

(1) Typical approach for LH_2 production using H_2SMR requires three steps: (I) gaseous H_2 production, (II) purification and (III) H_2 liquefaction. The cryogenic separation process illustrated in Fig. 9 combines hydrogen purification and liquefaction by means of an integrated process that is more efficient and has lower capital costs.

(2) The cryogenic separation process takes advantage of the differences in relative volatility of the components in the gas mixture. In principle, the physical separation can be more precise and the distillation parameters can be more easily controlled to produce the desired hydrogen purity. Another reason for integrated LH_2 production and cryogenic separation is that most of the cryogenic energy input to the process can be recovered via a network of heat exchangers—minimizing the amount of energy wasted.

In the membrane separation, the energy required for the compression cannot be fully recovered. Therefore, the overall input energy for gaseous hydrogen production must be somewhat greater than that in a cryogenic separation process. If LH_2 is required as a final product, additional cryogenic energy is needed to liquefy the gaseous H_2, resulting in an even greater energy input. In summary, the cryogenic separation process can be more efficient than a membrane separation process when liquid hydrogen is required as a final product. Detailed analyses and flow diagrams of LH_2 production from methane and landfill gas are given elsewhere [14].

3.3. *Overall process efficiency*

Since hydrogen sulfide in the feed stream is considered to be a contaminant, its combustion heat is not included in the H_2SMR process efficiency calculations. The first and second law efficiencies can then be defined by the following equations:

$$\eta_{1\text{st}}\,(\%) = \frac{\text{combustion heat for } H_2 \text{ produced} + LH_2 \text{ cooling energy}}{\text{total combustion heat for } CH_4 + \text{total process heat}} \times 100 \quad \text{(h)}$$

$$\eta_{2\text{nd}}\,(\%) = \frac{\text{useful work for } H_2 \text{ produced}}{\text{total combustion heat for } CH_4 + \text{total process heat}} \times 100 \quad \text{(i)}$$

Fig. 13 illustrates the first and second law efficiencies as functions of the inlet hydrogen sulfide to methane ratios ($1/x$) for the two H_2SMR cases depicted in Figs. 9 and 11. These results indicate that H_2SMR is an efficient process for the production of both gaseous and liquid hydrogen, with first law and second law efficiencies of more than 80% and 50%, respectively. These efficiencies decrease as the feed ratio x decreases. In addition, H_2SMR has the added benefit of converting a toxic waste (*i.e.* H_2S) to a useful fuel (*i.e.* H_2) and a commodity chemical (*i.e.* CS_2).

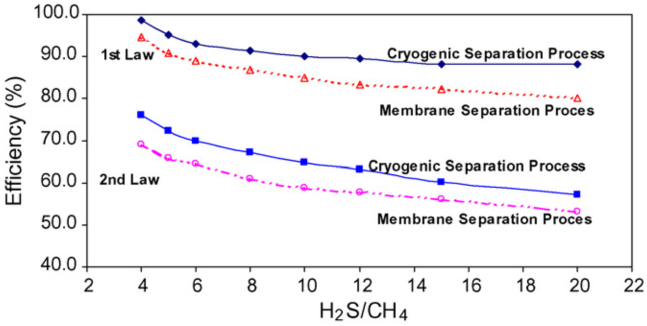

Fig. 13. H_2SMR process efficiencies.

4. Conclusions

A process for the production of hydrogen from high sulfur gas has been described and fully analyzed. The process involves hydrogen sulfide reformation of methane, generating hydrogen and carbon disulfide. Since carbon lay down during hydrogen sulfide methane reformation (H_2SMR) can deactivate the catalyst, thermodynamic analysis was carried out to identify reaction conditions under which no coking occurs. The thermochemical equilibrium calculations reveal the existence of pinch point temperatures at which all of the methane reacts with hydrogen sulfide to produce hydrogen and carbon disulfide and yielding no solid carbon by-product. At the pinch point temperatures or higher, the total amount of energy required by H_2SMR is the lowest. The thermodynamics of H_2SMR show that the process can be divided into three temperature zones: (1) CH_4 pyrolysis, (2) both CH_4 pyrolysis and H_2SMR and (3) H_2SMR plus partial H_2S pyrolysis. The pinch point temperatures are located in the transition temperature range between zone 2 and 3. At the pinch point temperatures the total heat requirement decreases dramatically from the high values expected for the H_2SMR and CH_4 pyrolytic processes to lower values associated with mainly H_2SMR. Results from the chemical process simulation flowsheets indicate that the H_2SMR process can be utilized for the production of liquid hydrogen via cryogenic separation unit operation. Compared to membrane separation processes, the cryogenic process has higher first and second law efficiencies exceeding 80% and 50%, respectively.

Acknowledgment

Authors are grateful for the financial support provided by the National Aeronautics and Space Administration (NASA), Glenn Research Center (GRC) under Grant no. NAG3-2751.

References

[1] R.H. Hugman, E.H. Vidas, P.S. Springer, 1993, GRI-93/0456.
[2] A. T-Raissi, Proceedings of the US DOE Hydrogen Program Review Meeting, Baltimore, MD, 2001.
[3] A.L. Kohl, R.B. Nielsen, Gas Purification, 5th ed., Gulf Publishing Company, Houston, Texas, 1997, pp. 670–865.
[4] S. Mizuta, W. Kondo, K. Fujii, Ind. Eng. Chem. Res. 30 (1991) 1601–1608.
[5] J. Zaman, A. Chakma, Fuel Process. Technol. 41 (1995) 159–198.
[6] D.W. Kalina, E.T. Maas Jr., Int. J. Hydrogen Energy 10 (3) (1985) 157–162.
[7] D.W. Kalina, E.T. Maas Jr., Int. J. Hydrogen Energy 10 (3) (1985) 163–167.
[8] C.A. Linkous, C. Huang, R.J. Fowler, J. Photochem. Photobiochem. A: Chem. 168 (3) (2004) 153–160.
[9] C. Huang, C.A. Linkous, US Patent no. 784,393 (2007).

[10] C. Huang, S. Franklyn, K.K. Ramasamy, C.A. Linkous, N.Z. Muradov, A. T-Raissi, Preprints of Symposia—American Chemical Society, Division of Fuel Chemistry, vol. 52, no. 2, 2007, pp. 678–679.
[11] C. Huang, A. T-Raissi, J. Power Sources 163 (2007) 645–652.
[12] C. Huang, A. T-Raissi, J. Power Sources 163 (2007) 637–644.
[13] E.J. Erekson, Gasoline from natural gas by sulfur processing, Final Technical Report, Institute of Gas Technology, DOE/PC/92114-T12 (1999).
[14] C. Huang, A. T-Raissi, J. Power Sources 173 (2007) 950–958.